HEPATOBILIARY-PANCREAS

Comparison of the diagnostic performance of 2D and 3D MR elastography in staging liver fibrosis

Mengsi Li[1] · Hao Yang[1,2] · Yong Liu[3] · Linqi Zhang[1] · Jingbiao Chen[1] · Ying Deng[1] · Yuanqiang Xiao[1] · Jie Zhu[1] · Zhuoya Yi[1] · Bing Hu[1] · Sichi Kuang[1] · Bingjun He[1] · Kevin J. Glaser[4] · Meng Yin[4] · Sudhakar K. Venkatesh[4] · Richard L. Ehman[4] · Jin Wang[1]

Abstract

Objectives To compare the diagnostic performance and image quality of state-of-the-art 2D MR elastography (MRE) and 3D MRE in the basic application of liver fibrosis staging.

Methods This retrospective study assessed data from 293 patients who underwent 2D and 3D MRE examinations. MRE image quality was assessed with a qualitative 2-point grading system by evaluating artifacts. Two experienced analysts independently measured mean liver stiffness values. The interobserver agreement of liver stiffness measurement was assessed by the intraclass correlation coefficient (ICC). The area under the receiver operating characteristic curve (AUC) was used to assess the diagnostic performance of 2D and 3D MRE and blood-based markers for fibrosis staging using the pathology-proven liver fibrosis stage as the gold standard.

Results The image quality provided by 3D MRE was graded as significantly higher than that obtained with the 2D MRE method ($p < 0.01$). Interobserver agreement in liver stiffness measurements was higher for 3D MRE (ICC: 3D 0.979 vs 2D 0.955). The AUC values for discriminating $\geq$ F1, $\geq$ F2, $\geq$ F3, and F4 fibrosis for 3D MRE (0.89, 0.92, 0.95, and 0.93) were similar to those for 2D MRE (0.89, 0.91, 0.94, and 0.92). Both the 2D and 3D MRE methods provided superior accuracy to the blood-based biomarkers, including APRI, FIB-4, and Forns index, especially for $\geq$ F2, $\geq$ F3, and F4 fibrosis stages (all $p < 0.01$).

Conclusions While 3D MRE offers certain advantages and opportunities for new applications of MRE, current widely deployed 2D MRE technology has comparable performance in the basic application of detecting and staging liver fibrosis.

Key Points
• *2D MRE and 3D MRE have comparable diagnostic performance in detecting and staging liver fibrosis.*
• *3D MRE has superior image quality and interobserver agreement compared to 2D MRE.*

Keywords MR elastography · 2D and 3D MRE · Fibrosis

Mengsi Li and Hao Yang contributed equally to this work.

✉ Jin Wang
  wangjin3@mail.sysu.edu.cn

[1] Department of Radiology, The Third Affiliated Hospital, Sun Yat-Sen University (SYSU), No. 600, Tianhe Road, Guangzhou, Guangdong 510630, People's Republic of China

[2] Department of Radiology, Sun Yat-sen Memorial Hospital, Sun Yat-sen University (SYSU), No. 107, Yanjiangxi Road, Guangzhou, Guangdong 510120, People's Republic of China

[3] Department of Pathology, The Third Affiliated Hospital, Sun Yat-Sen University (SYSU), No. 600, Tianhe Road, Guangzhou, Guangdong 510630, People's Republic of China

[4] Department of Radiology, Mayo Clinic College of Medicine, Mayo Clinic, Rochester, MN, USA

Abbreviations

2D	Two-dimensional
3D	Three-dimensional
APRI	Aspartate transaminase-to-platelet ratio index
AUC	Area under the curve
BMI	Body mass index
FIB-4	Fibrosis index based on four factors
FOV	Field of view
GRE	Gradient recalled echo
ICC	Intraclass correlation coefficient
IQR	Interquartile range
MRE	Magnetic resonance elastography
NPV	Negative predictive value

PPV   Positive predictive value
ROC   Receiver operating characteristic
ROI   Regions of interest
SE-EPI Spin-echo echo-planar imaging

Introduction

Among patients with chronic liver disease, assessing liver fibrosis is of great importance for treatment and determining prognosis. Early hepatic fibrosis is reversible, and patients with advanced hepatic fibrosis require ongoing screening for portal hypertension and hepatocellular carcinoma [1]. Although liver biopsy is considered the gold standard for staging fibrosis, it has several limitations, such as invasiveness, risk of complications [2], sampling errors, and interobserver variation in interpretation [3]. Noninvasive methods used to assess liver fibrosis have been developed, such as biochemical tests, ultrasound elastography, and magnetic resonance elastography (MRE). Of these methods, MRE is gaining acceptance as the most accurate noninvasive tool for evaluating liver fibrosis [4–6].

The current regulatory-approved implementations of MRE available from major MRI manufacturers utilize standardized two-dimensional (2D) MRE acquisition parameters and processing techniques (https://qibawiki.rsna.org/images/f/f6/MRE-QIBA_Profile-2019-06-06-CONSENSUS-maintenance.pdf). The shear wave driver devices in these systems are designed to generate waves that mainly propagate transversely in the liver, enabling the valid assessment of the wave field in individual transverse sections. These data are processed with a 2D inversion algorithm to generate quantitative images of liver stiffness. The commercially available versions of MRE also encode motion only in the through-plane direction as this has been found to be adequate for the calculation of liver stiffness in 2D MRE. These design decisions facilitated the initial introduction of MRE by MRI manufacturers. The early versions of 2D MRE were implemented with gradient recalled echo (GRE) sequences [7], and many published studies have demonstrated that the technique has excellent diagnostic performance in detecting and staging liver fibrosis [8–11]. After initial GRE, MRE sequences based on spin-echo echo-planar imaging (SE-EPI) have been shown to reduce technical failures due to the rapid T2* decay in the liver, and are now widely deployed, particularly on 3.0-T MRI systems [6, 12–18].

A more advanced implementation of MRE technology for the assessment of the liver is three-dimensional MRE (3D MRE). Using this technique, the shear wave field is imaged and analyzed in three dimensions to calculate stiffness within a volume rather than in individual 2D sections. 3D MRE acquisition is usually based on a multislice SE-EPI sequence. By more precisely acquiring and processing wave data in all directions of propagation, in principle, 3D MRE is more accurate than 2D MRE [19]. In addition, 3D MRE sequences can be designed to capture cyclic motion in all three directions at each voxel, allowing the use of more sophisticated 3D inversion algorithms that provide additional tissue characterization biomarkers, such as the individual components of the complex shear modulus [20].

Conceptually, it is reasonable to anticipate that, due to its improved accuracy and the ability to assess a larger volume of liver, 3D MRE may have higher diagnostic performance than 2D MRE in the basic clinical application of detecting and staging liver fibrosis. However, conventional 2D MRE is currently widely available and has well-established diagnostic performance in this application. The limited studies performed thus far have not conclusively established whether 3D MRE is superior or equivalent to 2D MRE in detecting and staging liver fibrosis [9, 10, 12].

Therefore, the goal of this study was to evaluate the comparative diagnostic performance of state-of-the-art SE-EPI-based 2D MRE and advanced 3D MRE in a larger study.

Materials and methods

This single-center, cross-sectional, retrospective study was approved by our institutional review board, with a waiver of the informed consent requirement. We included all consecutive adult patients who visited the Department of Radiology at our hospital for liver MRI examination with suspected diffuse diseases or focal lesions of the liver between December 2014 and October 2020.

Population

According to the inclusion/exclusion criteria summarized in Fig. 1, patients were included if they (a) were aged at least 18 years, (b) underwent 2D and 3D SE-EPI MRE examinations, and (c) underwent a histologic examination within 1 month of the MRE scanning. In total, 456 patients were initially eligible for the study. The exclusion criteria included (a) antiviral or other treatments before the MRE examination ($n = 130$), (b) a loose or disconnected driver ($n = 17$), or (c) inadequate specimens or inconsistent pathological results ($n = 13$). Three MRE examinations failed due to severe motion artifacts in elderly patients with chronic obstructive pulmonary disease who were unable to perform breath holds. While using SE-EPI MRE, none of the MRE examinations failed due to T2* effects. Ultimately, 293 patients were selected for this cohort study. The patients' demographic characteristics, epidemiological data, biochemical test results, and pathology information were retrospectively collected from the electronic medical
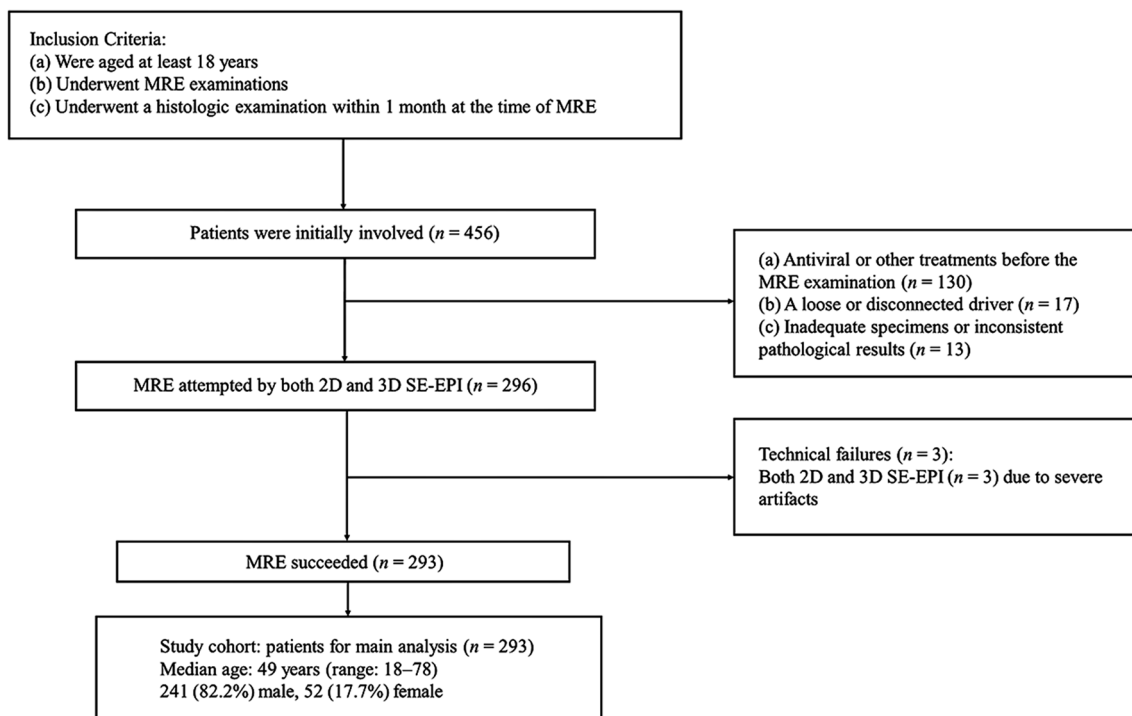
Fig. 1 Flow chart for the inclusion and exclusion criteria in the study cohort. SE-EPI, spin-echo echo-planar imaging; MRE, magnetic resonance elastography

records of the Hospital Information System. The biochemical tests included the platelet count, prothrombin time, international normalized ratio, gamma glutamyl transpeptidase, total cholesterol, albumin, and aspartate aminotransferase and alanine aminotransferase levels. Three serum fibrosis biomarkers, i.e., the aspartate transaminase-to-platelet ratio index (APRI), fibrosis index based on four factors (FIB-4), and Forns index, were calculated.

MRE acquisition

All MRE examinations were performed at a 60-Hz shear wave frequency, using standard, commercially available equipment. We used SE-EPI MRE sequences, which reduce the occurrence of technical failure compared with earlier, gradient echo-based MRE acquisition sequences. The patients fasted for at least 4 h before the MRE examinations. A passive pneumatic driver was placed over the right lobe of the liver centered at the level of the xiphisternum. Continuous mechanical vibrations at 60 Hz were generated using an active acoustic driver located outside of the scan room and were transmitted through polyvinyl chloride tubing to the passive driver to produce continuous shear waves in the liver [21]. The MR protocols also included routine anatomic MRI and dynamic contrast enhancement of the liver. All MRE examinations were performed before the intravenous administration of contrast agents [22] using a 3-T clinical scanner (Discovery MR750,

GE Healthcare) with an 8-channel, phased-array, torso coil. In the context of this study, we used two MRE protocols. The 2D

Table 1 Parameters for the 2D and 3D MRE

Parameters	2D MRE	3D MRE
Acquisition matrix	80 × 80	80 × 80
TE (ms)	51.4–52.5	51.7–52.8
TR (ms)	1000–1067	1334
EPI-shots	1	1
No. of breath holds × breath hold time (s)	1 × 16	3 × 21
FOV (cm)	38–44	38.7–44.8
No. of slices × slice thickness (mm)	4 × 8	32 × 3.5
Gap between slices (mm)	2	0
Parallel imaging acceleration factor	2	2
Phase offsets	4	3
Receiver bandwidth	500 kHz	500 kHz
% FOV in phase-encoding direction	75–100	100
Flow compensation	Yes	Yes
Superior-inferior spatial presaturation bands	Yes	Yes
Motion sensitivity (μm/radian)	7.86	7.86
Motion encoding directions	± Z	± X, Y, Z

TE, echo time; *TR*, repetition time; *FOV*, field of view; *2D*, two-dimensional; *3D*, three-dimensional; *EPI*, echo-planar imaging; *MRE*, magnetic resonance elastography

SE-EPI MRE protocol acquired 4 slices using the following parameters: standard through-plane motion encoding direction; repetition time, 1000–1067 ms; echo time, 51.4–52.5 ms; EPI-shots, 1; matrix, 80 × 80; slice thickness, 8 mm; slice spacing, 2 mm; field of view (FOV): 38–44 cm; parallel imaging acceleration factor, 2; phase offsets, 4; % FOV in phase-encoding direction, 75–100; and scan time, 16 s. The 3D MRE protocol acquired 32 slices with the following parameters: encoding for three orthogonal motion directions; repetition time, 1334 ms; echo time, 51.7–52.8 ms; EPI-shots, 1; matrix 80 × 80; slice thickness, 3.5 mm; slice spacing, 0 mm; FOV: 38.7–44.8 cm; parallel imaging acceleration factor, 2; phase offsets, 3; % FOV in phase-encoding direction, 100; and scan time, 63 s [12]. These protocols required a single breath hold for the 2D MRE 4-slice acquisition and three breath holds for the 32-slice 3D MRE acquisition. The 4 sections acquired with 2D MRE were axial images located in the widest part of the liver. The 32 transverse sections of the 3D MRE acquisition usually spanned most of the liver volume. After processing, four sections were selected from the 3D MRE examination to match the 4 sections acquired with 2D MRE. The primary parameters of the 2D and 3D MRE examinations are summarized in Table 1.

2D and 3D MRE image quality analysis

All images were analyzed by two radiologists with experience in liver imaging. A primary observer (H.Y., 4 years of experience with MRE interpretation) and a secondary observer (J.B.C., 5 years of experience with MRE interpretation) assessed and scored the image quality of the 2D and 3D MRE acquisitions by consensus based on the elastogram, phase image, and wave propagation images. None of the examinations in the final 293-patient cohort was assessed as nondiagnostic. Therefore, the image quality was assigned as "acceptable" or "excellent" [12]. "Excellent" image quality was defined as the absence of artifacts or the presence of artifacts at edges, boundaries, or fissures that can easily be avoided while defining large regions of interest (ROIs) to measure liver stiffness. The examinations that were classified as "acceptable" had minor artifacts in the images, but ROIs of a reasonable size could still be defined for the stiffness measurement. The artifacts were recognized based on experience and knowledge that they are caused by wave interference, structural discontinuities, local failure in phase unwrapping, and cardiovascular or respiratory motion.

2D and 3D MRE stiffness measurement

The two analysts, who were blinded to the histologic information, independently measured liver stiffness. The analysts manually defined the ROIs in the right lobes of the liver using the MRE magnitude, wave, and stiffness images. The MRE analysis was performed according to the methods described in the "consensus profile" of MRE developed and published by the Quantitative Imaging Biomarkers Alliance (https://qibawiki.rsna.org/images/f/f6/MRE-QIBA_Profile-2019-06-06-CONSESUS-maintenance.pdf). This process involved defining the ROIs as follows: (1) The ROIs were drawn manually in the largest possible area of the liver parenchyma in which coherent shear waves were visible while excluding the major blood vessels observed on the MRE magnitude images. (2) Areas of incoherent waves and regions immediately under the passive driver were avoided, and the ROIs excluded areas close to the liver boundary and contained a minimum of 500 pixels per slice [23, 24]. (3) The ROIs were confined to the right lobe whenever possible. After the ROIs were drawn, the mean stiffness of each section was recorded, and the mean value of all sections was computed and weighed by the ROI size. After assessing the interobserver agreement, the measurements in each examination by the two analysts were averaged for further analysis [25].

Assessment of pathologic specimens

Liver fibrosis was assessed in all patients by either clinically indicated liver biopsy or a histological analysis of the background parenchyma after hepatic resection for focal liver lesions. In our institution, liver biopsy was performed under ultrasound guidance using an intercostal approach with a 16- or 18-gauge automated edge-cutting biopsy needle (Bard Magnum) under local anesthesia. Liver biopsy specimens with a length < 15 mm and those containing < 6 portal tracts (except for cirrhosis) were strictly excluded. In the hepatic resection cases, a sampling site exceeding 1.5 cm^2 was selected as far away (at least 1 cm) from the focal liver lesion margin as possible to avoid potential changes in inflammation, increased vascularity, and fibrosis induced by focal liver lesions [26]. Then, all specimens were fixed in formalin, embedded in paraffin, stained with hematoxylin-eosin, and counterstained with either reticulin or Masson's stain. Two hepatopathologists with more than 10 years of clinical experience analyzed all specimens by consensus. The pathologists were blinded to the radiological and clinical data. Disagreements were resolved by consensus.

The fibrosis staging and inflammatory activity were evaluated semiquantitatively according to the METAVIR scoring system [27]. The fibrosis stage was assigned using an ordinal scale from 0 to 4 as follows: no fibrosis (F0); mild fibrosis, portal fibrosis without septa (F1); substantial fibrosis, portal fibrosis with few septa (F2); moderate to advanced fibrosis, numerous septa without cirrhosis (F3); and cirrhosis (F4). Inflammatory activity was graded on a scale ranging from 0 to 3 as follows: A0, no inflammation; A1, mild inflammation; A2, moderate inflammation; and A3, severe inflammation.

Table 2 Baseline characteristics of the 293 patients

Characteristic	Patients ($n = 293$)
Demographics	
Sex (M/F)	241/52
Age (years), mean (s.d.; range)	49 (12; 18–78)
Body mass index (kg/m^2), mean (s.d.; range)	22.8 (3.3; 10.5–33.8)
Biochemical data	
Alanine aminotransferase (IU/L), median (IQR)	35 (23–54)
Aspartate aminotransferase (IU/L), median (IQR)	33 (25–47)
Gamma glutamyl transpeptidase (IU/L), median (IQR)	59 (35–122.5)
Total bilirubin (IM/L), median (IQR)	12.8 (9.5–18.3)
Platelet count, 10^3/mm^3, median (IQR)	177 (125–241)
Albumin (g/L), median (IQR)	41.3 (38.4–44.3)
International normalized ratio, median (IQR)	1.05 (1.00–1.11)
Liver specimens	
Biopsy	220 (75.1%)
Liver resection	73 (24.9%)
Etiology	
HBV	242 (82.6%)
HCV	11 (3.8%)
HBV+HCV	2 (0.7%)
Autoimmune hepatitis	10 (3.4%)
Drug induced	5 (1.7%)
Alcohol induced	3 (10.3%)
NAFLD	15 (5.1%)
Primary sclerosing cholangitis	5 (1.7%)
Fibrosis	
F0	22 (7.5%)
F1	55 (18.8%)
F2	59 (20.1%)
F3	65 (22.2%)
F4	92 (31.4%)
Inflammation grade	
A0	11 (3.8%)
A1	122 (41.6%)
A2	64 (21.8%)
A3	96 (32.8%)

HBV, hepatitis B virus; *HCV*, hepatitis C virus; *NAFLD*, nonalcoholic fatty liver disease; *IQR*, interquartile range

Statistical analysis

Values (age and body mass index (BMI)) showing a normal distribution were expressed as the means ($\pm$ SDs), while data showing a non-normal distribution were expressed as the medians with interquartile ranges (IQRs). The Wilcoxon signed-rank test was used to compare the image quality of 2D and 3D MRE. The interobserver agreement regarding the liver stiffness measurement was assessed using the intraclass correlation coefficient (ICC) and the differences in the ICC of the two MRE techniques were evaluated using a Q test. The differences in liver stiffness in each fibrosis stage between 2D and 3D MRE were analyzed using independent-sample t tests. The correlation in liver stiffness between the two MRE sequences was assessed by Pearson's correlation coefficient, and the correlations between the inflammation grades and liver stiffness were calculated using Spearman's correlation analysis. Receiver operating characteristic (ROC) curve analyses were performed to assess the diagnostic performance of MRE and serum fibrosis markers in the differentiation of each fibrosis stage. The statistical analyses were performed using SPSS version 24 (SPSS Inc.) and R version 3.4.3 (R-Foundation). A p value < 0.05 was considered indicative of a significant difference.

Table 3 Success rate, image quality, ICC of liver stiffness measurement, and liver stiffness in each fibrosis stage of the 2D and 3D MRE

	2D MRE	3D MRE	p value
Success rate (n = 296)			N/A
Success	293 (99.0%)	293 (99.0%)	
Failure	3 (1.0%)	3 (1.0%)	
Image quality (n = 293)			0.000
Acceptable	61 (20.8%)	3 (1.0%)	
Excellent	232 (79.2%)	290 (99.0%)	
ICC of liver stiffness measurement (n = 293)			0.001
ICC (95% CI)	0.955 (0.944, 0.964)	0.979 (0.974, 0.983)	
Liver stiffness of fibrosis stage (kPa) (n = 293)			
No fibrosis (F0, n = 22)	2.48 ± 0.32	2.17 ± 0.28	0.001
Mild fibrosis (F1, n = 55)	2.73 ± 0.37	2.34 ± 0.30	0.000
Moderate fibrosis (F2, n = 59)	3.12 ± 0.61	2.65 ± 0.37	0.000
Advanced fibrosis (F3, n = 65)	4.18 ± 1.09	3.45 ± 0.84	0.000
Cirrhosis (F4, n = 92)	5.94 ± 1.76	5.03 ± 1.89	0.002

ICC, intraclass correlation coefficient; *MRE*, magnetic resonance elastography; *N/A*, not applicable

Results

Patient characteristics

A flowchart detailing the inclusion and exclusion of patients in this study is shown in Fig. 1. In the final study group of 293 patients, the median patient ages were 50 years (IQR, 42–58 years) among the men (241, 82.3%) and 50 years (IQR, 39–60 years) among the women (52, 17.7%). In total, 73 (24.9%) patients underwent surgery (local tumor resection, 57; hemihepatectomy, 11; and liver transplantation, 5) and 220 (75.1%) patients underwent ultrasound-guided percutaneous liver biopsies at our institution. Hepatitis B virus infection had the highest prevalence at 82.6% (242/293). The numbers of patients with fibrosis stages 0, 1, 2, 3, and 4 were 22, 55, 59, 65, and 92, respectively. The numbers of patients with inflammation grade 0, 1, 2, and 3 were 11, 122, 64, and 96, respectively. Moderate correlations were observed between

Fig. 2 A 51-year-old male patient with stage F3 fibrosis. Mean liver stiffness values with 2D and 3D MRE were 3.65 kPa and 3.35 kPa, respectively. 2D and 3D MRE stiffness maps (**a** and **b** respectively) had no prominent artifacts and the image quality of both was classified as "excellent." **c** 2D wave image showed excellent wave illumination in the liver. **d** Magnitude image
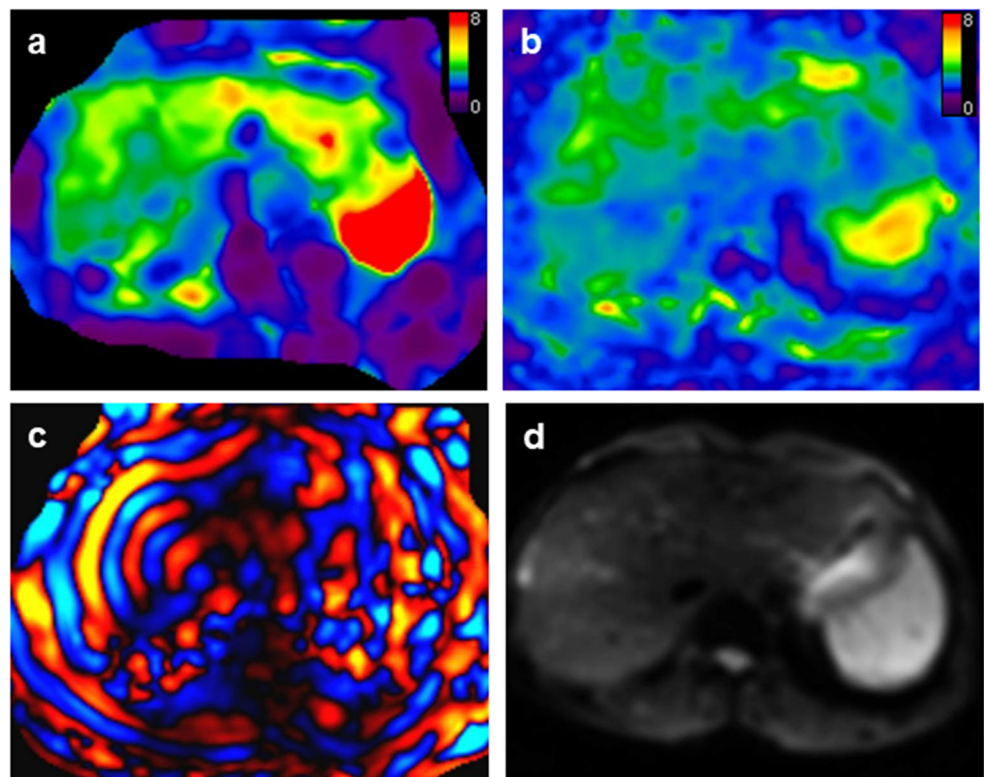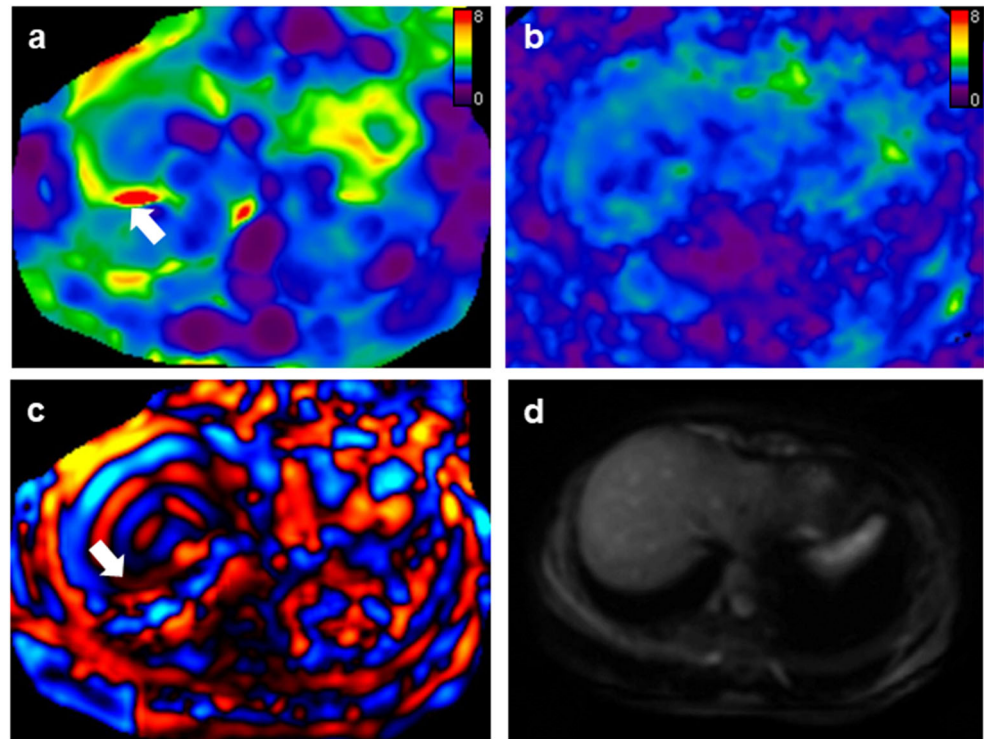
Fig. 3 A 27-year-old female patient with positive hepatitis B infection and F0 fibrosis. Mean liver stiffness values with 2D and 3D MRE were 2.54 kPa and 2.29 kPa, respectively. **a** 2D MRE had an artifact (white arrow) in the right liver lobe and the examination was classified as "acceptable." **b** 3D MRE had no apparent artifacts and the examination was rated as "excellent." **c** 2D wave image demonstrated wave interference (white arrow) causing the artifact. **d** Magnitude image

the inflammation grades and liver stiffness (2D MRE: $r = 0.694$, $p < 0.001$; 3D MRE: $r = 0.703$, $p < 0.001$). The patient demographic characteristics, epidemiological data, biochemical test results, and pathology information are summarized in Table 2.

Image quality assessment and liver stiffness measurement

The success rate and image quality grades of the 2D and 3D MRE techniques are summarized in Table 3. Both 2D and 3D

Fig. 4 A 27-year-old female patient with positive hepatitis B infection and F0 fibrosis. Mean liver stiffness values with 2D and 3D MRE were 2.39 kPa and 2.37 kPa, respectively. **a** 2D MRE exam showed artifacts typically resulting from transmitted cardiac impulse (white arrows). The image quality was classified as "acceptable." **b** 3D MRE had no apparent artifacts and the examination was rated as "excellent." **c** 2D wave image. **d** Magnitude image
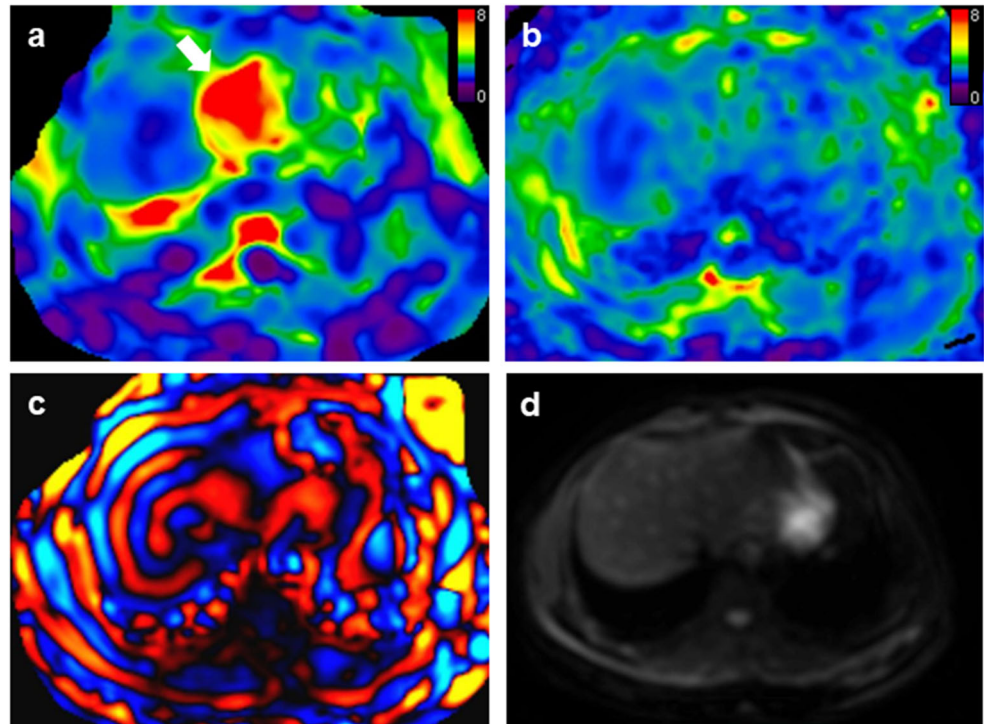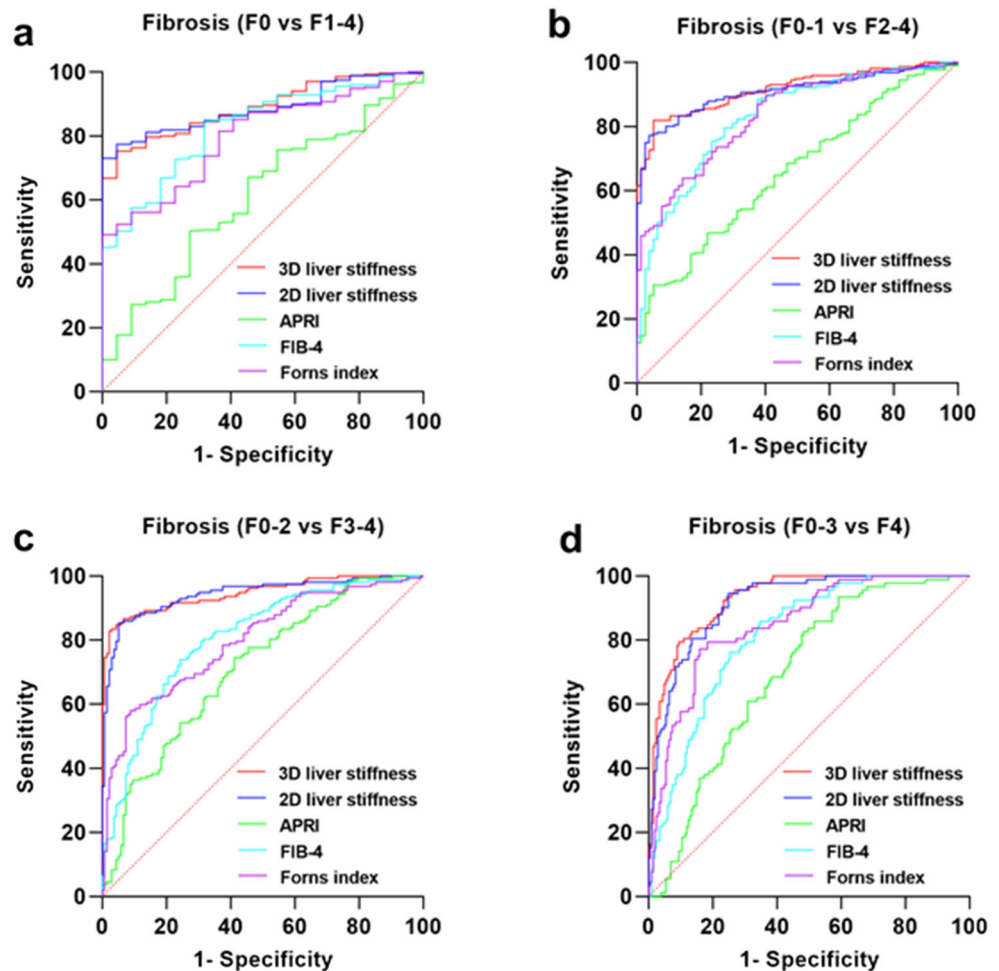
Fig. 5 Receiver operating characteristic (ROC) curves for 2D MRE, 3D MRE, and laboratory-based fibrosis biomarkers. **a** F0 vs F1–4. **b** F0–1 vs F2–4. **c** F0–2 vs F3–4. **d** F0–3 vs F4. APRI, aspartate transaminase-to-platelet ratio index; FIB-4, fibrosis index based on four factors

MRE had identically high success rates (293/296, 99.0%). Using 2D MRE, 232 examinations (79.2%) were classified as "excellent" quality, and 61 examinations (20.8%) were classified as "acceptable." Using 3D MRE, 290 examinations (99.0%) were of "excellent" quality, and only 3 (1.0%) examinations were of lower quality in the "acceptable" category. The higher image quality assessment of the 3D MRE examinations was statistically significant ($p < 0.001$). Representative 2D and 3D MRE images are shown in Figs. 2, 3, and 4.

There was a strong interobserver agreement in the measured liver stiffness of both 2D and 3D MRE. The ICC of 3D MRE (0.979 (95% CI: 0.974, 0.983)) was significantly higher than that of 2D MRE (0.955 (95% CI: 0.944, 0.964)) ($p = 0.001$). The results are summarized in Table 3.

Performance of 2D MRE, 3D MRE, and serum fibrosis biomarkers in liver fibrosis staging

In the entire 293-patient cohort, the areas under the ROC curves (AUCs) for discriminating the $\geq$ F1, $\geq$ F2, $\geq$ F3, and $\geq$ F4 fibrosis stages using 2D MRE were 0.89, 0.91, 0.94, and 0.92, respectively, and those using 3D MRE were 0.89,

0.92, 0.95, and 0.93, respectively. The differences in the AUC values between 2D MRE and 3D MRE were not statistically significant (all $p > 0.05$). Both the 2D and 3D MRE methods demonstrated significantly higher diagnostic accuracy than the laboratory-based tests, including the APRI, FIB-4, and Forns index, in classifying significant fibrosis ($\geq$ F2), advanced fibrosis ($\geq$ F3), and cirrhosis (F4) (all $p < 0.01$; Fig. 5).

The liver stiffness measurements using 2D MRE and 3D MRE were highly correlated ($r = 0.950$, $p < 0.001$). The 2D MRE stiffness cutoff values for various stages of fibrosis were higher than those of 3D MRE (F0 vs F1–4, 2D: 2.99 kPa, 3D: 2.54 kPa; F0–1 vs F2–4, 2D: 3.25 kPa, 3D: 2.65 kPa; F0–2 vs F3–4, 2D: 3.64 kPa, 3D: 3.15 kPa; F0–3 vs F4, 2D: 3.67 kPa, 3D: 3.64 kPa).

These results are summarized in Table 4.

Discussion

This retrospective single-center study focused on comparing the diagnostic performance of 2D MRE and 3D MRE in the

Table 4 Diagnostic performance of 2D MRE, 3D MRE, and serum fibrosis biomarkers for detecting liver fibrosis stage

	Cutoff value	AUC (95% CI)	Sensitivity (95% CI)	Specificity (95% CI)	PPV (95% CI)	NPV (95% CI)
Cirrhosis (F4)						
3D liver stiffness in kPa	3.64	0.93 (0.90–0.96)	79.4 (69.4–86.8)	90.6 (85.4–94.1)	79.4 (69.4–86.8)	90.6 (85.4–94.1)
2D liver stiffness in kPa	3.67	0.92 (0.89–0.95)	94.6 (87.2–98.0)	75.1 (68.5–80.8)	63.5 (54.8–71.4)	96.8 (92.3–98.8)
APRI	0.21	0.70*** (0.64–0.76)	82.6 (73.0–89.4)	51.7 (44.6–58.8)	43.9 (36.5–51.7)	86.7 (79.0–92.0)
FIB-4	1.60	0.82*** (0.77–0.86)	85.9 (76.7–92.0)	65.2 (58.1–71.7)	53.0 (44.7–61.2)	91.0 (84.8–94.9)
Forns index	9.00	0.85*** (0.80–0.90)	77.2 (67.0–85.0)	84.1 (78.1–88.7)	68.9 (59.0–77.5)	89.0 (83.4–92.9)
Advanced fibrosis (≥ F3)						
3D liver stiffness in kPa	3.15	0.95 (0.92–0.97)	82.8 (75.8–88.2)	97.8 (93.2–99.4)	97.7 (93.1–99.4)	83.1 (76.2–88.4)
2D liver stiffness in kPa	3.64	0.94 (0.92–0.97)	85.4 (78.6–90.3)	94.9 (89.3–97.7)	95.0 (89.7–97.8)	84.9 (78.0–90.0)
APRI	0.21	0.71*** (0.65–0.77)	74.5 (66.8–81.0)	58.8 (50.1–67.1)	67.6 (60.0–74.4)	66.7 (57.4–74.9)
FIB-4	1.60	0.81*** (0.76–0.86)	73.9 (66.2–80.4)	75.7 (67.5–82.5)	77.9 (70.2–84.1)	71.5 (63.3–73.6)
Forns index	9.00	0.80*** (0.75–0.85)	58.0 (49.8–65.7)	91.2 (84.8–95.2)	88.4 (80.2–93.6)	65.3 (58.0–71.9)
Significant fibrosis (≥ F2)						
3D liver stiffness in kPa	2.65	0.92 (0.89–0.95)	81.9 (76.0–86.7)	94.8 (86.5–98.3)	97.8 (94.1–99.3)	65.2 (55.5–73.8)
2D liver stiffness in kPa	3.25	0.91 (0.88–0.94)	77.3 (71.0–82.6)	96.1 (88.3–99.0)	98.2 (94.5–99.5)	60.2 (50.9–68.8)
APRI	0.47	0.66*** (0.59–0.73)	30.6 (24.6–37.2)	94.8 (86.5–98.3)	94.3 (85.3–98.2)	32.7 (26.7–39.4)
FIB-4	1.24	0.83** (0.78–0.88)	79.6 (73.5–84.7)	72.7 (61.2–82.0)	89.1 (83.6–93.0)	56.0 (45.7–65.8)
Forns index	8.14	0.84** (0.79–0.89)	63.9 (57.1–70.2)	85.7 (75.5–92.3)	92.6 (86.9–96.1)	45.8 (37.6–54.3)
Any fibrosis (≥ F1)						
3D liver stiffness in kPa	2.54	0.89 (0.84–0.94)	74.9 (69.2–79.9)	95.5 (75.1–99.8)	99.5 (96.9–100.0)	23.6 (15.5–34.0)
2D liver stiffness in kPa	2.99	0.89 (0.84–0.93)	73.1 (67.3–78.2)	100.0 (81.5–100.0)	100.0 (97.6–100.0)	23.2 (15.4–33.2)
APRI	0.27	0.61*** (0.49–0.72)	50.2 (44.1–56.3)	72.7 (49.6–88.4)	95.8 (90.6–98.3)	10.6 (6.4–16.9)
FIB-4	0.85	0.83 (0.75–0.90)	84.5 (79.5–88.5)	68.2 (45.1–85.3)	97.0 (93.7–98.7)	26.3 (15.9–39.9)
Forns index	8.46	0.80* (0.72–0.88)	49.1 (43.0–55.2)	100.0 (81.5–100.0)	100.0 (96.5–100.0)	13.8 (9.0–20.3)

Significant difference between MRE methods and serum fibrosis biomarkers. $*p < 0.05$; $**p < 0.01$; $***p < 0.001$

MRE, magnetic resonance elastography; *APRI*, aspartate transaminase-to-platelet ratio index; *FIB-4*, fibrosis index based on four factors; *AUC*, area under the curve; *PPV*, positive predictive value; *NPV*, negative predictive value

important clinical task of staging liver fibrosis. The results indicate that, despite theoretical advantages, such as the potential for improved measurement accuracy, 3D MRE did not outperform 2D MRE in staging liver fibrosis. Both techniques had excellent performance in discriminating ≥ F1, ≥ F2, ≥ F3, and F4 fibrosis, consistent with previously published studies [9, 28–32]. Both techniques also substantially outperformed the laboratory-based biomarkers evaluated in this study. The lower cutoff values observed using 3D MRE are consistent with previous studies that have generally demonstrated that liver stiffness measurements obtained at 60 Hz using 3D MRE are consistently lower than 2D MRE measurements [9, 33]. This effect occurs partially because 2D MRE can overestimate stiffness if the observed shear waves do not propagate exactly parallel to the plane of the section. The effects of image noise and larger ROI sizes have also been suggested to be influential in the difference [9, 12]. The cutoff values for all stages obtained using 2D MRE in previous studies using a 3.0-T MRE system have been modestly higher than those observed in this

study [28, 30]. We speculate that this discrepancy may be attributable to significant differences in the underlying etiologies of fibrosis in these studies [11, 34]. The cutoffs observed for 3D MRE were similar to those in a previous study [9].

The wide availability of the 2D MRE technique used in this study, coupled with the advantage of requiring only one breath hold, provides a good justification for its ongoing use in liver fibrosis staging in routine clinical practice. However, 3D MRE has potential advantages that were not evaluated in this study. Repeatability is an important performance characteristic when a test is used longitudinally. The repeatability of 2D MRE is excellent [35], but due to its technical advantages, image quality superiority, and higher interobserver agreement observed in this study, the repeatability of 3D MRE may be substantially better. In addition, 3D MRE offers additional biomarkers that have been shown to hold promise for increasing the diagnostic utility of MRE [20]. Inflammatory activity was found to be modestly correlated with liver stiffness in 2D and 3D MRE measurements, consistent with the results of

another published study [9]. Nevertheless, 2D MRE– and 3D MRE–assessed liver stiffness showed excellent performance in staging liver fibrosis in this study.

There are several limitations to our study. The retrospective nature and requirement of liver biopsy may have resulted in a selection bias and heterogeneity in the patient population. The mixed etiologies of liver diseases in our cohort might affect comparisons and studies involving a single etiology are warranted in the future. Some patients had focal liver lesions, which potentially could influence the stiffness of adjacent, apparently uninvolved liver tissue. Furthermore, this study did not include an in-depth analysis of inflammation.

In conclusion, this comparison of the performance of 2D MRE and 3D MRE in staging liver fibrosis demonstrated that both techniques have high and equivalent diagnostic performance. However, the 3D MRE technique provided superior image quality and higher interobserver agreement.

Declarations

Guarantor The scientific guarantor of this publication is Jin Wang.

Conflict of interest The authors of this manuscript declare no relationships with any companies whose products or services may be related to the subject matter of the article.

Statistics and biometry No complex statistical methods were necessary for this paper.

Informed consent Written informed consent was waived by the Institutional Review Board.

Ethical approval Institutional Review Board approval was obtained.

Methodology
• retrospective
• diagnostic or prognostic study
• performed at one institution

References

1. Castera L (2012) Noninvasive methods to assess liver disease in patients with hepatitis B or C. Gastroenterology 142:1293–1302

2. Seeff LB, Everson GT, Morgan TR et al (2010) Complication rate of percutaneous liver biopsies among persons with advanced chronic liver disease in the HALT-C trial. Clin Gastroenterol Hepatol 8: 877–883

3. Regev A, Berho M, Jeffers LJ et al (2002) Sampling error and intraobserver variation in liver biopsy in patients with chronic HCV infection. Am J Gastroenterol 97:2614–2618

4. Lefebvre T, Wartelle-Bladou C, Wong P et al (2019) Prospective comparison of transient, point shear wave, and magnetic resonance elastography for staging liver fibrosis. Eur Radiol 29:6477–6488

5. Hoodeshenas S, Yin M, Venkatesh SK (2018) Magnetic resonance elastography of liver: current update. Top Magn Reson Imaging 27: 319–333

6. Venkatesh SK, Yin M, Ehman RL (2013) Magnetic resonance elastography of liver: technique, analysis, and clinical applications. J Magn Reson Imaging 37:544–555

7. Yin M, Talwalkar JA, Glaser KJ et al (2007) Assessment of hepatic fibrosis with magnetic resonance elastography. Clin Gastroenterol Hepatol 5:1207–1213

8. Zhan C, Kannengiesser S, Chandarana H, Fenchel M, Ream J, Shanbhogue KP (2019) MR elastography of liver at 3 Tesla: comparison of gradient-recalled echo (GRE) and spin-echo (SE) echo-planar imaging (EPI) sequences and agreement across stiffness measurements. Abdom Radiol (NY) 44:1825–1833

9. Shi Y, Xia F, Li QJ et al (2016) Magnetic resonance elastography for the evaluation of liver fibrosis in chronic hepatitis b and c by using both gradient-recalled echo and spin-echo echo planar imaging: a prospective study. Am J Gastroenterol 111:823–833

10. Kim YS, Jang YN, Song JS (2018) Comparison of gradient-recalled echo and spin-echo echo-planar imaging MR elastography in staging liver fibrosis: a meta-analysis. Eur Radiol 28:1709–1718

11. Chang W, Lee JM, Yoon JH et al (2016) Liver fibrosis staging with MR elastography: comparison of diagnostic performance between patients with chronic hepatitis b and those with other etiologic causes. Radiology 280:88–97

12. Wang J, Glaser KJ, Zhang T et al (2018) Assessment of advanced hepatic MR elastography methods for susceptibility artifact suppression in clinical patients. J Magn Reson Imaging 47:976–987

13. Wagner M, Corcuera-Solano I, Lo G et al (2017) Technical failure of MR elastography examinations of the liver: experience from a large Single-Center study. Radiology 284:401–412

14. Felker ER, Choi KS, Sung K et al (2018) Liver MR elastography at 3 T: agreement across pulse sequences and effect of liver R2* on image quality. AJR Am J Roentgenol 211:588–594

15. Wagner M, Besa C, Bou AJ et al (2016) Magnetic resonance elastography of the liver: qualitative and quantitative comparison of gradient echo and spin echo echoplanar imaging sequences. Invest Radiol 51:575–581

16. Mariappan YK, Dzyubak B, Glaser KJ et al (2017) Application of modified spin-echo-based sequences for hepatic MR elastography: evaluation, comparison with the conventional gradient-echo sequence, and preliminary clinical experience. Radiology 282:390–398

17. Choi SL, Lee ES, Ko A et al (2020) Technical success rates and reliability of spin-echo echo-planar imaging (SE-EPI) MR elastography in patients with chronic liver disease or liver cirrhosis. Eur Radiol 30:1730–1737

18. Kim DW, Kim SY, Yoon HM, Kim KW, Byun JH (2020) Comparison of technical failure of MR elastography for measuring liver stiffness between gradient-recalled echo and spin-echo echo-planar imaging: a systematic review and meta-analysis. J Magn Reson Imaging 51:1086–1102

19. Glaser KJ, Manduca A, Ehman RL (2012) Review of MR elastography applications and recent developments. J Magn Reson Imaging 36:757–774

20. Allen AM, Shah VH, Therneau TM et al (2020) The role of three-dimensional magnetic resonance elastography in the diagnosis of nonalcoholic steatohepatitis in obese patients undergoing bariatric surgery. Hepatology 71:510–521

21. Wang J, Shan Q, Liu Y et al (2019) 3D MR elastography of hepatocellular carcinomas as a potential biomarker for predicting tumor recurrence. J Magn Reson Imaging 49:719–730

22. Plaikner M, Kremser C, Zoller H et al (2019) Does gadoxetate disodium affect MRE measurements in the delayed hepatobiliary phase? Eur Radiol 29:829–837

23. Yin M, Glaser KJ, Talwalkar JA, Chen J, Manduca A, Ehman RL (2016) Hepatic MR elastography: clinical performance in a series of 1377 consecutive examinations. Radiology 278:114–124

24. Dzyubak B, Venkatesh SK, Manduca A, Glaser KJ, Ehman RL (2016) Automated liver elasticity calculation for MR elastography. J Magn Reson Imaging 43:1055–1063

25. Kottner J, Audige L, Brorson S et al (2011) Guidelines for Reporting Reliability and Agreement Studies (GRRAS) were proposed. J Clin Epidemiol 64:96–106

26. Morisaka H, Motosugi U, Ichikawa S et al (2018) Magnetic resonance elastography is as accurate as liver biopsy for liver fibrosis staging. J Magn Reson Imaging 47:1268–1275

27. Bedossa P, Poynard T (1996) An algorithm for the grading of activity in chronic hepatitis C. The METAVIR Cooperative Study Group. Hepatology 24:289–293

28. Yoshimitsu K, Mitsufuji T, Shinagawa Y et al (2016) MR elastography of the liver at 3.0 T in diagnosing liver fibrosis grades; preliminary clinical experience. Eur Radiol 26:656–663

29. Loomba R, Cui J, Wolfson T et al (2016) Novel 3D magnetic resonance elastography for the noninvasive diagnosis of advanced fibrosis in NAFLD: A prospective study. Am J Gastroenterol 111:986–994

30. Imajo K, Kessoku T, Honda Y et al (2016) Magnetic resonance imaging more accurately classifies steatosis and fibrosis in patients with nonalcoholic fatty liver disease than transient elastography. Gastroenterology 150:626–637

31. Huwart L, Sempoux C, Vicaut E et al (2008) Magnetic resonance elastography for the noninvasive staging of liver fibrosis. Gastroenterology 135:32–40

32. Bohte AE, de Niet A, Jansen L et al (2014) Non-invasive evaluation of liver fibrosis: a comparison of ultrasound-based transient elastography and MR elastography in patients with viral hepatitis B and C. Eur Radiol 24:638–648

33. Morisaka H, Motosugi U, Glaser KJ et al (2017) Comparison of diagnostic accuracies of two- and three-dimensional MR elastography of the liver. J Magn Reson Imaging 45:1163–1170

34. Castera L, Forns X, Alberti A (2008) Non-invasive evaluation of liver fibrosis using transient elastography. J Hepatol 48:835–847

35. Serai SD, Obuchowski NA, Venkatesh SK et al (2017) Repeatability of MR elastography of liver: a meta-analysis. Radiology 285:92–100